ARTICLE

DOI: 10.1590/2317-4889201920180083

BJGEO
Brazilian Journal of Geology

Reappraisal of the Sumé Complex: geochemistry and geochronology of metaigneous rocks and implications for Paleoproteorozoic subduction-accretion events in the Borborema Province, NE Brazil

Edilton José dos Santos[1†], Lauro Cézar Montefalco de Lira Santos[2*]

Abstract

The Alto Moxotó Terrane represents the largest exposure of Paleoproterozoic rocks in the central Borborema Province. Several medium- to high-grade metamorphic units are described in the terrane, however geochronological data are still scarce, and the main periods of crust build-up and recycling are poorly known. In this study, we investigate the nature and age of metagranitic and metamafic-ultramafic rocks in the type area of the Sumé Complex. U-Pb zircon data from a metasyenogranite yields a concordant age of 1.97 Ga, which is in contrast with the previously published age of the complex (c. 640 Ma). In addition, Sm-Nd isotope signature indicates Paleoproterozoic to Mesoarchean sources that coupled with negative εNd(t) values suggest reworking of a preexisting crust. Whole-rock geochemical data indicate that metamafic rocks are similar to those already described in the terrane, corresponding to island-arc tholeiites, whereas the metagranitic rocks share similarities with magmas that were generated in an evolved stage of an orogenic setting. The obtained results are coherent with a long-lived Paleoproterozoic accretionary-collisional event (c. 2.1 – 1.9 Ga) described in the Borborema Province, which is correlative with Paleoproterozoic (c. 2.2 – 2.0 Ga) basement inliers/terranes from Pan-African Fold belts..

KEYWORDS: Sumé Complex; Accretion tectonics; Alto Moxotó Terrane; Borborema Province; Western Gondwana.

INTRODUCTION

The role of orogenic-collisional events in generation, preservation and reworking of continental crust in Precambrian provinces is one of the most debated topics in earth sciences (*e.g.*, Hawkesworth & Kemp 2006, Hawkesworth *et al.* 2017). A critical point lies on how similar or not Early Earth and Phanerozoic thermal regimes are. For instance, geochemical and isotope record of granites, mafic rocks, supracrustal sequences and high-grade metamorphic assemblages, including granulites and eclogites, suggest that mid- to late Precambrian and Phanerozoic convergent tectonics could have been quite similar in most cases (Rudnick 1995, Cawood *et al.* 2009, 2013).

In contrast, early Paleoproterozoic and Archean regimes seem to be different in a number of aspects, including partial melting rates, speed of crustal growth and potential sources for melt generation (Martin *et al.* 2005, Brown 2006). Nevertheless, it is consensus that, in most Phanerozoic and Precambrian orogens, injection of high amounts of juvenile magmas via accretionary wedges generates new crust, whereas subduction-collisional orogens strongly rework the previous and ancient formed crust (Cawood *et al.* 2009, Hong & Kao 2015). In extremely deformed orogens, the nature of major crust building and reworking events needs careful and critical analysis, given that early crustal processes might have been hidden by younger subduction, collisional or rifting events. Another critical issue lies on the identification and description of basement inliers or exotic terranes that can be considerably older than the final tectonic stabilization. The recognition and detailed description of previously formed crust are hard tasks, but it can provide crucial information, once that they can represent travelling fragments that are missing in large cratonic blocks (*e.g.*, Zhao *et al.* 2004, Meert 2012).

In Western Gondwana, several Neoproterozoic orogens are interpreted as the result of oceanic subduction followed by continent-continent collision of cratons and minor crustal blocks. Most of these orogens/provinces are characterized by Ediacaran to Cambrian arc-related lithotectonic units, that are widespread and preserved. Thus, the investigation of magmatic and metamorphic events provides reliable clues on processes related to the final assembly of Gondwana (Vaughan *et al.* 2005, De Wit *et al.* 2008, Brito Neves *et al.* 2014).

In the Neoproterozoic Borborema Province (NE Brazil, central portion of Western Gondwana), recent geochemical-isotopic investigations, focused on petrological and tectonic aspects of Archean and Paleoproterozoic basement inliers or exotic terranes, demonstrate the complexity

[1]Serviço Geológico do Brasil – Recife (PE), Brazil.

[2]Department of Geology, Universidade Federal de Pernambuco – Recife (PE), Brazil. E-mail: lauromontefalco@gmail.com

[†]*In memoriam.*

*Corresponding author.

and variety of crustal processes that took place prior to its present configuration (*e.g.*, Brito Neves *et al.* 2014, Caxito *et al.* 2016, Ganade *et al.* 2017, Santos *et al.* 2017b, Costa *et al.* 2018). Within its central portion, the Alto Moxotó Terrane/Domain (AMT) is considered one of the most preserved Paleoproterozoic crustal segments of the entire province (Brito Neves *et al.* 2000). Among its numerous units, Medeiros and Torres (2000) described an important lithostratigraphic sequence that occupies a large area of the terrane, named as Sumé Complex. This unit is characterized by a large variety of rock types such as gneisses, banded iron formation (BIF), ultramafic rocks, granulites and calc-silicates rocks with innumerous tangential orthogneisses varying to granitic to leuco-tonalitic/anorthositic compositions. Their initial stratigraphic placement without using isotopic tools refer to Paleo- to Mesoproterozoic eras.

Silva *et al.* (2002) dated homogeneous zircon crystals (U-Pb sensitive high-resolution ion microprobe—SHRIMP) from a foliated hornblende granodiorite with porphyroclastic texture, interpreted as part of the Sumé Complex, yielding a date of 640 ± 6 Ma. Such age was interpreted as the crystallization age of the rock, whereas a zircon xenocryst of ~841 Ma delineates an early crustal inheritance (Silva 2006). This data led some authors to distinguish a number of Neoproterozoic rocks throughout the terrane. Recently, Santos *et al.* (2015) demonstrated that part of the Sumé Complex corresponds in fact to a major Paleoproterozoic association, including metamorphic, ultramafic, mafic and felsic rocks, marking two tectonically important contrasting events in the region:

1. Siderian and Rhyacian accretion-collision;
2. Statherian-Calymmian within-plate magmatism.

Such older associations are inconsistent with the previously obtained Ediacaran age. Therefore, the origin of the Sumé Complex is still an open question.

In this paper, we present new U-Pb age, Sm-Nd isotope and whole-rock geochemistry data of metagranitoids and associated metamafic rocks from the Sumé Complex. Our main goals are:

1. to investigate the magma protoliths, including the associated tectonic setting;
2. to elucidate the proper stratigraphic position of the studied rocks and consequently the Sumé Complex (*i.e.*, Neoproterozoic *vs.* Paleoproterozoic);
3. to demonstrate the importance of this crustal segment to the understanding of the Borborema Province Precambrian evolution.

GEOLOGICAL SETTING, FIELD RELATIONSHIPS AND PETROGRAPHY

The Sumé Complex is inserted in the AMT, a dominantly Paleoproterozoic domain that underlies a NE-SW segment of the central Borborema Province. The province itself comprises a major portion of NE South American platform, comprising several individual lithotectonic domains that record tectono-magmatic and metamorphic histories spanning Archean to Ediacaran-Cambrian times (Almeida *et al.* 1981, Brito Neves *et al.* 2000). As several other mobile belts of Western Gondwana, it has been built by tectonic convergence of major cratonic blocks (*i.e.*, São Francisco-Congo and São Luís-West Africa cratons), during Neoproterozoic and Cambrian times (Brito Neves *et al.* 2014).

According to Van Schmus *et al.* (2011), the Borborema Province can be tectonically divided into the Northern, Transversal and Southern sub-provinces, which are limited by two major E-W shear zones: the Patos lineament, to the north; and Pernambuco lineament, to the south (Fig. 1). Up to now, the Neoproterozoic evolution of the Transversal sub-province is in the heart of a major debate, involving two main models:

1. accretion of crustal terranes during the Cariris Velhos (1000 – 920 Ma) and Brasiliano (650 – 540 Ma) orogenies (Brito Neves *et al.* 2000, Santos *et al.* 2010, 2017b, 2018);
2. intracontinental reworking of a larger Paleoproterozoic continent (Neves 2015, Neves *et al.* 2017).

In addition to the AMT, the Transversal sub-province is considered to consist of other four terranes/domains, namely São Pedro, Piancó-Alto Brígida or Cachoeirinha, Alto Pajeú and Rio Capibaribe (Santos & Medeiros 1999, Brito Neves *et al.* 2000, Basto *et al.* 2019). Within the AMT, two major units dominate, referred to as Floresta Complex or basement rocks (orthogneisses and migmatites with ages ranging from 2.2 to 2.1 Ga), and the Sertânia Complex (paragneisses, schists and migmatites dated at 2.1 – 2.0 Ga; Santos *et al.* 2004). However, Neves *et al.* (2017) reported Neoproterozoic detrital zircon ages (*c.* 700 Ma) from samples attributed to the Sertânia Complex.

Recently, Santos *et al.* (2015, 2017a) discussed the role of Archean and Paleoproterozoic rocks in the evolution of the AMT, which seems to be much more complex than the rest of the Transversal sub-province. It includes episodes of tonalite-trondhjemite-granodiorite (TTG) and sanukitoid generation, as well as several calc-alkaline metaluminous suites that record a long-lived Paleoproterozoic history of accretion and collision. Neves *et al.* (2015) achieved similar conclusions, studying different facies of orthogneisses and migmatitic rocks from the basement, as well as metamafic rocks.

The type area of the Sumé Complex comprises the central portion of the AMT and was defined in the work of the homonym geologic sheet (SB.24-Z-D-V; Medeiros & Torres 2000). This region is known by local and spaced occurrences of phosphate minerals, mainly apatite, hosted in skarn lenses (Nascimento *et al.* 2015). In the study area (Fig. 2), rocks of the Sumé Complex comprise interleaved granitic to metagranitic and metamafic-ultramafic rocks. The metagranitoids corresponds to monzogranites, syenogranites and minor alkali-feldspar granites (Fig. 3A). In the field, metamafic and metaultramafic rocks form pockets and rounded xenoliths within metagranitic members, suggesting magma mingling (Fig. 3B), whilst metagranitic rocks normally present a slightly to well developed foliation in response to regional stress, being whitish to pinkish-gray and pink, equi- to inequigranular, medium- to coarse-grained (Fig. 3C). Garnet-biotite paragneisses and leucossome-rich migmatites of the Sertânia Complex possibly host this set of metaplutonic rocks.

In thin sections, metagranitic rocks show granoblastic texture. Its mineralogy consists of subhedric to anhedric quartz (45–40%), euhedric to subhedric K-feldspar (35–30%) and euhedric, subhedric and anhedric plagioclase crystals (25–20%). In the most deformed samples, hipidioblastic to xenoblastic plagioclase crystals may occur, exhibiting myrmekite intergrowth, besides the presence of millimetric light brown biotite inclusions that can be partially bent. The latter is the main mafic mineral of these rocks. Hornblende and muscovite also occur in minor amounts, in addition to apatite and titanite. Euhedral, subhedral and rounded zircon crystals are common inclusions in biotite lamellae. Lastly, rounded to elliptic mafic clots, up to 1.5 cm in diameter, can be locally found following a discrete magmatic foliation or even deformed by regional tectonics, mostly composed of Ca-rich amphibole.

Metamafic and metaultramafic rocks are similar of those ones described as Carmo Suite by Santos *et al.* (2015). In the study area, metamafic members dominate and form fine to medium grained massif aggregates or lenses of amphibolites and metagabbros (Fig. 3D). Metraultramafic rocks are punctual, corresponding to pyroxenites (websterites and clinopyroxenites). The presence of vein-like structures with amphibole + chlorite ± epidote suggests hydrothermal alteration, interpreted as skarnitization of metamafic rocks.

Amphibolites and metagabros are characterized by greenish to pale yellow prismatic hornblende (55–45%), subidioblastic plagioclase (35–25%) and hipidioblastic to subidioblastic clinopyroxene (15–10%). Hornblende crystals are usually characterized by a micro-planar fabric constrained by the regional foliation (Fig. 3E). Mg-rich biotite can be present, forming less than 5% of the rock mode. The main structure of these rocks varies from massive to foliate. Lastly, euhedral ilmenite is the main opaque phase. Metapyroxenites consists of augite-hyperstene assemblages with slight uralitization to hornblende. In some samples, garnet might be present and develop corona textures around clinopyroxenes (CPX) and/or plagioclase crystals, suggesting retrograde metamorphism. Similar textures, including symplectites, are described in the Carmo Suite, which is the main Rhyacian mafic-ultramafic set of rocks of the AMT (Santos *et al.* 2015).

ANALYTICAL PROCEDURES

Laser ablation multi-collector induced coupled plasma mass spectrometry (LA-MC-ICP-MS) analyses were done from zircon grains separated from sample SC-05. This sample was collected just 2,5 km west of Sumé (see Fig. 2). Sample preparation and analysis were done in the facilities of the Geochronology Laboratory of

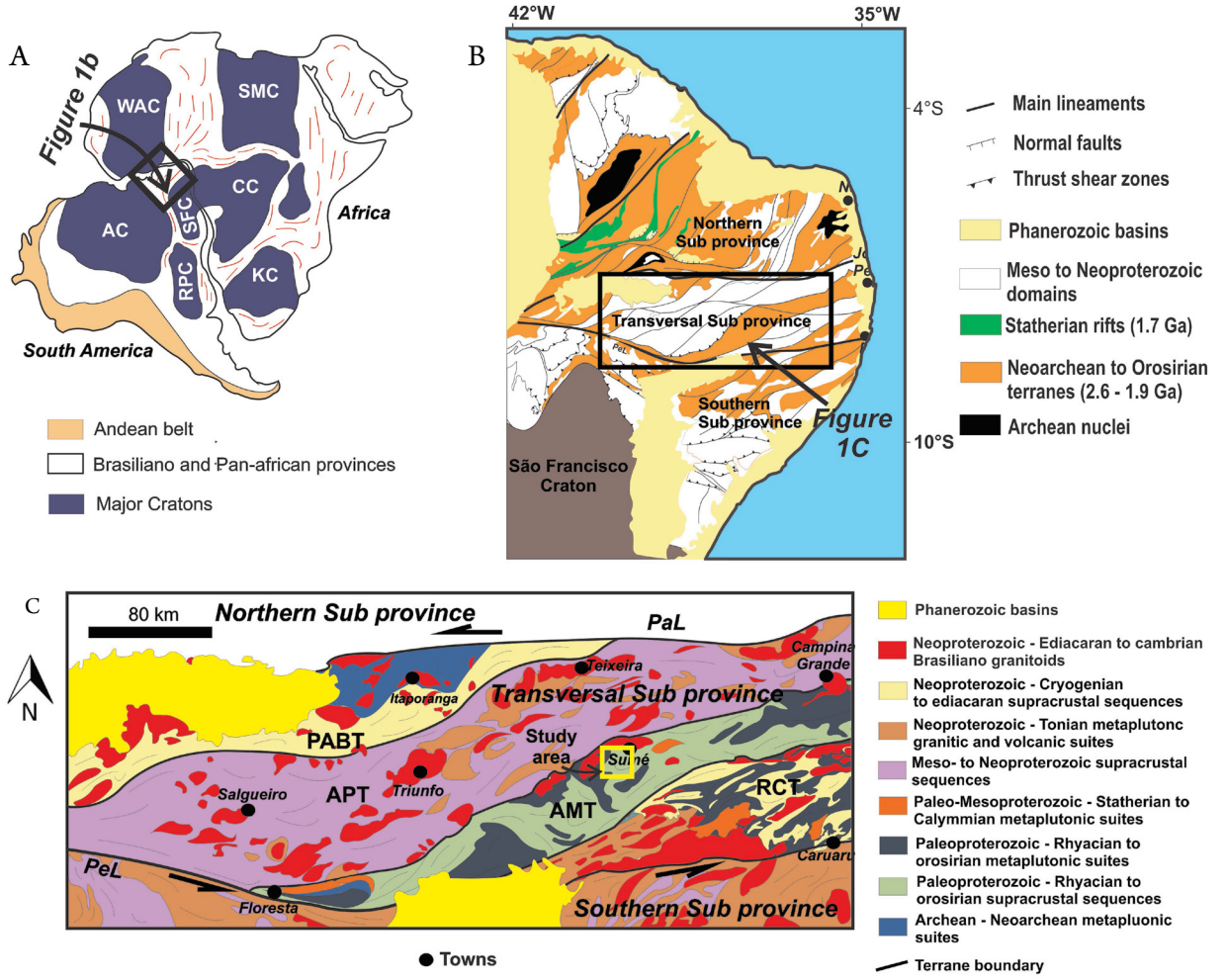

Figure 1. (A) Geodynamic context of the Borborema Province in pre-drift reconstruction for West Africa and northeastern South America; (B) tectonic framework of the Borborema Province; (B) simplified geological map of the Transversal sub-province and its domains with the study area highlighted.

Universidade de Brasília, Brazil. Standard procedures were followed, including crushing and grinding. The heavy minerals were separated using conventional gravimetric and magnetic methods. Zircon crystals were handpicked using binocular microscope and mounted on epoxy resin for isotope ratio acquisition. Data reduction was performed following Bühn *et al.* (2009) and Matteini *et al.* (2010). Back scattered electrons (BSE) and scanning electron microscopy (SEM) images were obtained prior to analysis to investigate the internal structure of the grains. Normalization was performed with internal GJ standard zircon (608 ± 1 Ma; Jackson *et al.* 2004), and

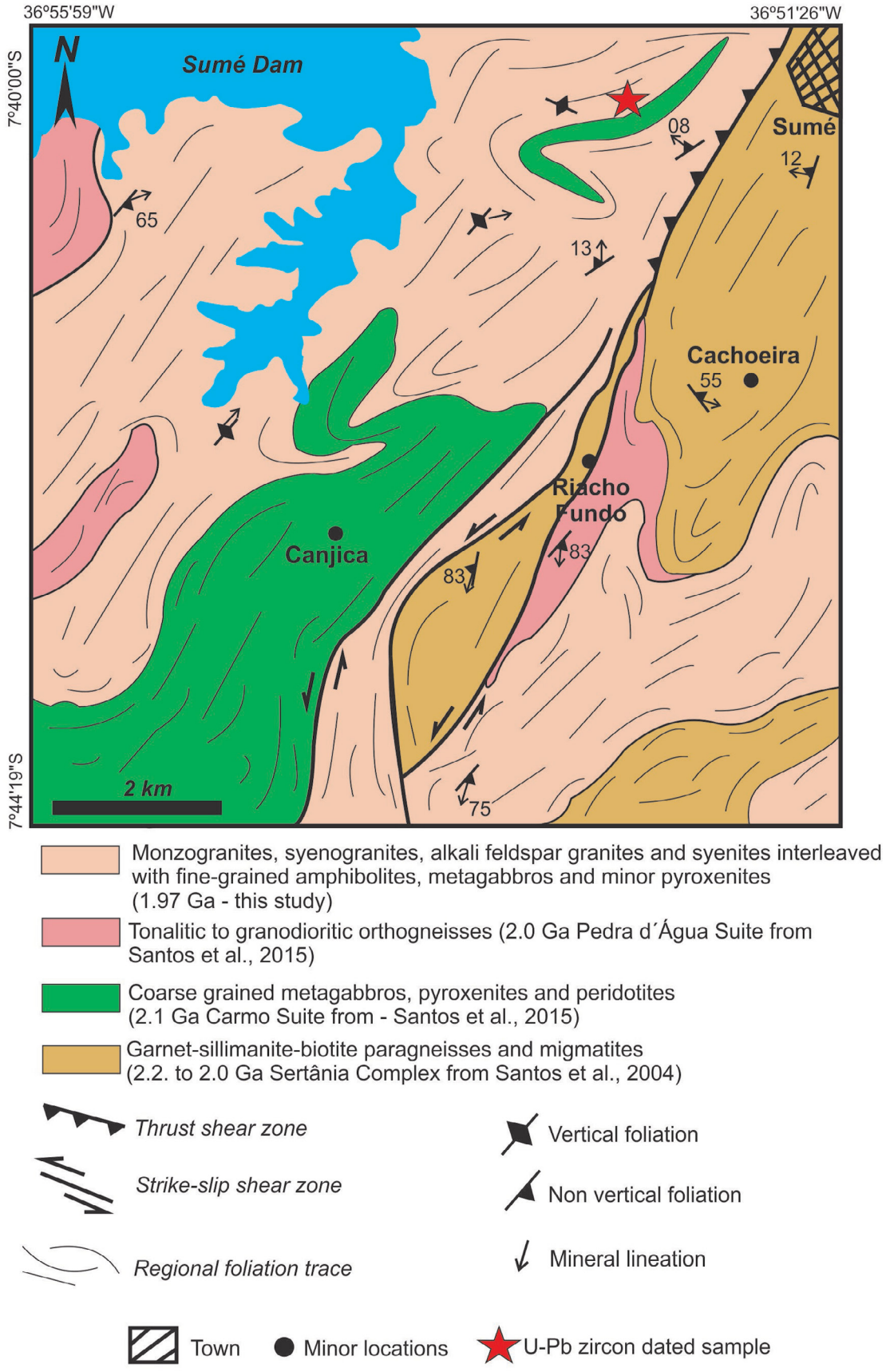

Figure 2. Simplified geological map of the study area showing the location of the selected sample for U-Pb zircon dating.

the age calculations were performed using in-house developed Excel spreadsheets.

Four samples were selected for the Sm-Nd data acquisition. A thermo triton mass spectrometer using degassed double Re filaments (99.995 % H. Cross®) at ~ 1,630°C were used in the Laboratory of the Center of Geochronological Researches (CPGeo), of the Universidade de São Paulo, and the applied methodology followed Magdaleno *et al.* (2017). The $^{143}Nd/^{144}Nd$ ratios were normalized to the value of $^{146}Nd/^{144}Nd = 0.7219$ [3], using an exponential law. Ion

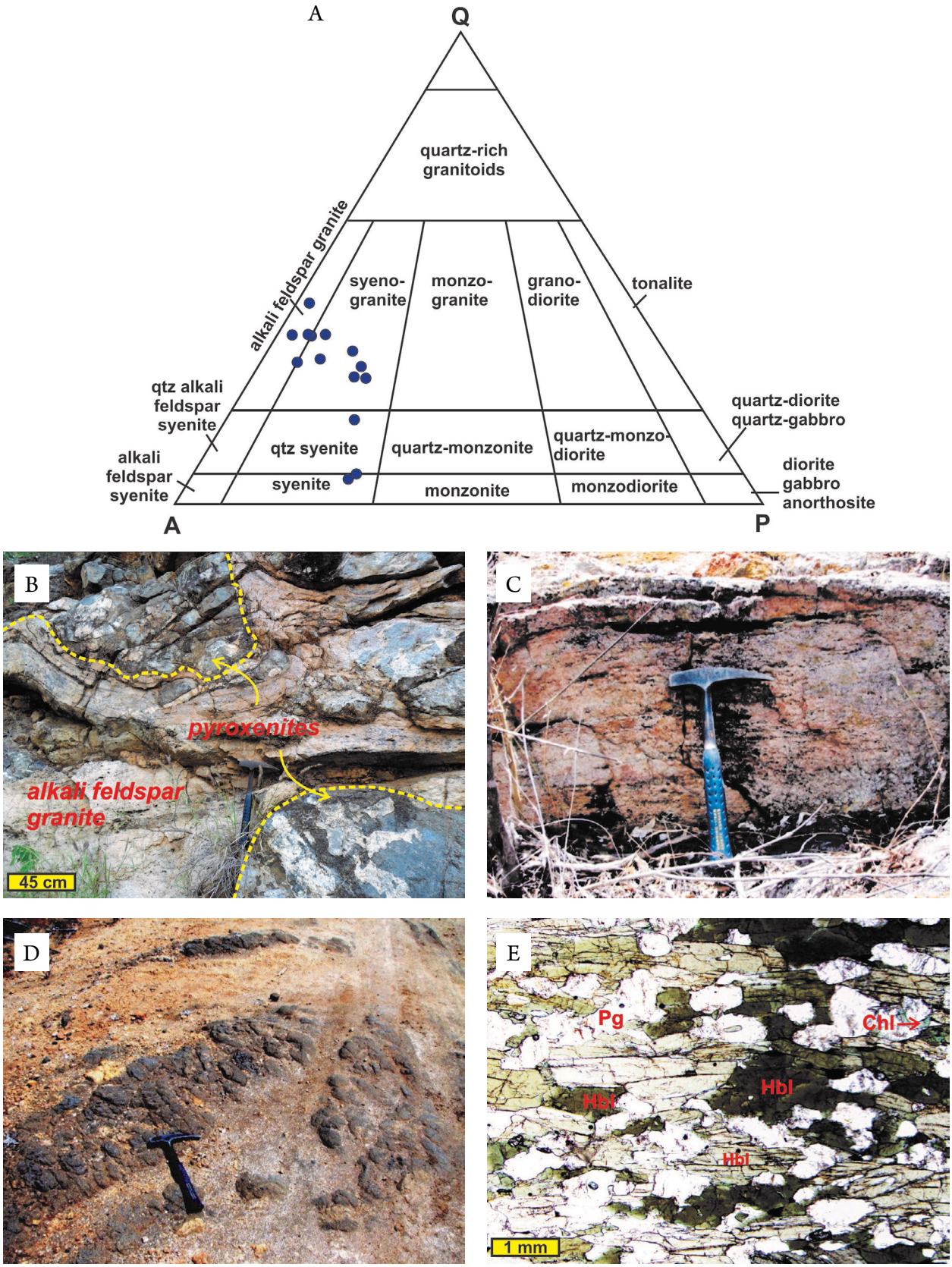

Figure 3. (A) Modal composition of the studied metagranitoids obtained by point counting; (B) rounded contact of alkali feldspar granite and pyroxenites, suggestive of preserved magma mingling; (C) foliated syenogranite of the outcrop selected for U-Pb dating; (D) metric layers of fine-grained massive metagabbros; (E) deformed and elongated hornblende crystals following the regional foliation imposed on an amphibolite sample.

beam intensities of ^{145}Nd for JNdi-1 standard were always higher than 1V.

Thirteen representative samples were selected for whole-rock chemical analysis, including six from metagranitic and seven from metamafic rock samples. They were analyzed in the ACME Laboratories (Canada). Major elements were analyzed using borate flux and read by X-ray flourescence (XRF). Trace elements, including rare earths, were determined by Li-metaborate fusion and plasma spectrometry with inductively coupled plasma mass spectrometry (ICP-MS) and atomic emission (ICP-AES).

RESULTS

U-Pb zircon age

The analyzed sample (SC-05) corresponds to a discretely foliated biotite metasyenogranite. The obtained isotopic ratios and apparent ages of each zircon grain are displayed in Table 1. Zircon grains from this sample range between 100 and 150 µm long and are mostly euhedral to subhedral. They are translucent, showing oscillatory zoning and thin rims, representing discrete metamorphic overgrowths. They also present Th/U ratios always higher than 0.1, which supports their magmatic origin. The data plotted in the Concordia diagram yield a concordant age of 1976 ± 23 Ma (95% of concordance), with a mean square weighted deviation (MSWD) of 0.21. The result is interpreted as the crystallization age of the rock protolith (Fig. 4).

Sm-Nd isotopes

Sm-Nd isotope analyses were performed on four representative samples of felsic and mafic rocks, and the results are presented in Table 2. The calculated Nd T_{DM} model ages following DePaolo (1981), range from 3.2 to 2.2 Ga, indicating involvement of Rhyacian to Mesoarchean sources. Figure 5 shows the εNd (t) evolution of the studied samples based on the U-Pb age of 1.97 Ga. These data are in agreement with calculated model ages, with values ranging from slightly to highly negative (*i.e.*, -0.08 to -10.44).

Whole-rock geochemistry

The summary of results of whole-rock geochemical data is presented in Table 3. The studied metagranitic rocks present high SiO_2 values that vary from 61.31 to 75.50%. Na_2O values are low to intermediate, ranging from 1.01 to 3.05%, whereas high K_2O contents vary from moderate to high (4.86 to 10.87%), which

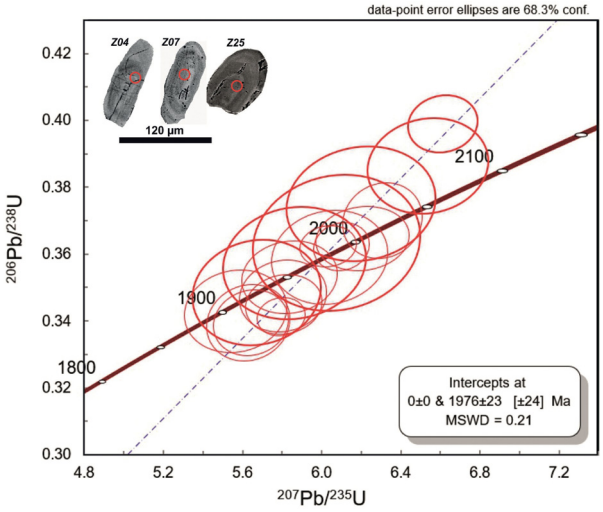

MSWD: mean square weighted deviation.

Figure 4. U-Pb concordia diagram and back scattered electrons (BSE) images of selected zircon crystals with spot positioning of sample SC-05 (biotite metasyenogranite).

Table 1. Summary of laser ablation inductively coupled plasma mass spectrometry (LA-ICP-MS) data of zircon grains from sample SC-05.

Grain spot	$^{207}Pb/^{206}Pb$ ratios	±(1σ)	$^{207}Pb/^{235}U$ ratios	±(1σ)	$^{206}Pb/^{238}U$ ratios	±(1σ)	$^{207}Pb/^{206}Pb$ ages	±(1σ)	$^{207}Pb/^{235}U$ ages	±(1σ)	$^{206}Pb/^{238}U$ ages	±(1σ)	Rho	Th/U ratio	Conc. (%)
Z07	0.12	1.96	5.57	3.08	0.34	2.37	1919.71	34.78	1910.91	26.51	1901.76	39.08	0.77	0.23	99.05
Z01	0.13	0.90	6.44	2.41	0.35	2.23	1957.53	16.00	2038.01	21.14	1928.00	37.17	0.93	0.29	96.31
Z30	0.12	1.10	5.65	2.21	0.34	1.92	1962.20	19.50	1924.35	19.07	1885.72	31.34	0.86	0.13	96.06
Z14	0.12	2.30	5.89	3.77	0.35	2.99	1925.52	40.59	1959.29	32.71	1939.67	50.05	0.79	0.13	100.13
Z05	0.13	0.85	5.92	1.39	0.34	1.10	1999.76	15.01	1963.52	12.09	1900.72	18.15	0.78	0.10	94.72
Z02	0.12	1.43	5.82	2.50	0.35	2.05	1971.14	25.30	1950.08	21.64	1924.87	34.05	0.82	0.59	97.59
Z06	0.13	1.37	5.99	2.19	0.35	1.70	1985.71	24.24	1973.78	19.04	1920.78	28.30	0.77	0.61	96.25
Z12	0.12	1.81	5.85	2.73	0.35	2.05	1953.32	32.02	1954.17	23.71	1951.20	34.45	0.76	0.12	99.85
Z04	0.12	2.64	5.86	4.08	0.36	3.11	1937.17	46.51	1955.61	35.37	1969.65	52.74	0.76	0.16	101.49
Z26	0.12	1.07	6.03	1.56	0.36	1.14	1964.25	19.01	1980.03	13.62	1994.45	19.52	0.71	0.10	101.50
Z11	0.12	1.94	6.06	3.22	0.36	2.57	1984.21	34.06	1984.47	28.05	1979.73	43.81	0.80	0.63	99.72
Z09	0.13	2.71	6.31	4.59	0.37	3.70	1974.23	47.59	2019.38	40.20	2010.02	63.85	0.81	17.98	101.22
Z25	0.12	0.80	6.10	1.53	0.36	1.31	1984.43	14.14	1989.95	13.35	1993.79	22.38	0.85	0.08	100.39
Z08	0.12	2.64	6.20	4.02	0.38	3.03	1952.29	46.48	2004.08	35.13	2053.59	53.22	0.76	0.11	105.13
Z27	0.12	1.80	6.20	2.50	0.36	1.75	1998.15	31.57	2004.93	21.90	2005.12	30.07	0.76	1.48	100.02
Z20	0.12	0.60	6.31	2.09	0.37	2.01	2005.95	10.57	2019.15	18.35	2030.50	34.96	0.96	0.24	101.14
Z15	0.12	1.92	6.54	3.10	0.39	2.44	1993.83	33.66	2050.78	27.30	2106.31	43.79	0.78	0.31	105.56
Z18	0.12	1.06	6.61	1.77	0.40	1.42	1958.01	18.79	2060.96	15.64	2164.66	26.16	0.80	0.30	110.51

Conc.: concordance.

are typical of evolved granitic and syenitic melts (Fig. 6A). This is in accordance with the obtained petrographic data. They plot in the calc-alkaline field on the AFM diagram and correspond to mainly metaluminous to slight peraluminous magmas (Figs. 6B and 6C). P_2O_5 and TiO_2 contents are low, ranging from 0.04 to 0.14% and 0.04 to 0.65%, respectively.

Metamafic samples are homogeneous and basic. SiO_2 content ranges from 46.8 to 51.0%. They also present low K_2O and Na_2O, which are 0.19 to 1% and 0.35 to 1.25%, respectively. These values are compatible with magmas that present gabbroic/basaltic composition (Fig. 6A). They are characterized by Al_2O_3 ranging from 3.18 to 10.26%, high CaO (18.5 – 22.8 %) and moderate to high contents of FeO, ranging from 5.3 to 10%, which is consistent with average values of magmas of the toleiitic series (Fig. 6B). TiO_2 and P_2O_5 ranges from 0.25 to 0.53 and 0.01 to 1.77%, respectively.

Trace elements of the metagranitic rocks show an enriched large ion litophile elements (LILE) pattern normalized to chondrite values of Nakamura (1974), exhibiting a discrete positive peak of Rb and depletion of high field strength elements (HFSE), such as Nb and Ta. Other characteristic negative anomalies are marked by P and Ti (Fig. 7A). Rare earth elements (REE) contents are moderate to high (ΣREE = 38.8 to 311.8), showing enrichment of light rare earth elements (LREE), indicated by the $(La/Yb)_N$ ratio values that range from 12.27 to 247.67, and associated Eu anomalies (Eu/Eu* ratios ranging between 0.39 to 1.43; Fig. 7B).

The incompatible element spidergram normalized to chondrite values of Nakamura (1974) for the mafic rocks presents moderate to low values of LILE and prominent negative Nb, Ta, Sr and P anomalies in most of the analyzed samples. A minor negative Ti anomaly and positive peaks of La and Ce are observed (Fig. 7C).

Total REE contents ranges from 65.3 to 414.7 ppm, and the REE patterns normalized to chondrite values of Nakamura (1974) are steep, showing moderate to high concentrations of LREE in relation to the heavy rare earth elements (HREE), with $(La/Yb)_N$ ratios ranging from 5.10 to 31.80. The samples are marked by a negative Eu anomaly (Eu/Eu* ~ 0.60 on average), except for sample SC37 (Fig. 7D).

In tectonic discriminant diagrams, metagranitic rocks share similarities with volcanic-arc related granites (Fig. 8A). The same is reflected on the classical discriminant diagram from Pearce *et al.* (1984), in which the studied samples plot both on volcanic arc granites (VAG) and syn-collisional (syn-COLG) fields (Fig. 8B). In addition, the distribution of trace elements for mafic members shows similar tectonic affinities. On the tectonic Hf/3-Th-Ta plot from Wood (1980), the samples share similarities with Arc-related basalts (Fig. 9A), also observed on the Nb/Th plot from Jenner *et al.* (1991) (Fig. 9B). Besides, on the DF1-DF2 diagrams proposed by Agrawal *et al.* (2008), samples correspond entirely to melts derived from island arc basalts (Figs. 9C and 9D).

DISCUSSION

Magmatism and tectonic setting

New petrographic, isotope and geochemical data of metagranoids and metamafic rocks provide clues on the tectonic evolution of the AMT, Borborema Province and early crustal processes of Western Gondwana. The metagranitoids derived from calc-alkaline and metaluminous to peraluminous magmas that are mostly monzo- and syenogranitic in composition. On the other hand, associated metamafic rocks are mostly amphibolites and fine-grained metagabros with toleiitic affinity. Lesser occurrences of metaultramafic rocks in the area are mostly represented by clinopyroxenites and websterites.

The dated sample of a metagranitic member yields an age of 1.97 Ga, which is interpreted as the crystallization age of its protolith. The Nd isotopic composition is variable for felsic and mafic members, being characterized by T_{DM} model ages, suggestive of the involvement of Paleoproterozoic and Archean components in the magma genesis, whilst the calculated $\varepsilon Nd_{(1.97)}$ is dominantly negative. These data indicate that the generation of the studied precursor magmas were coeval to crust reworking of the AMT. Indeed, rocks with slight similar age and isotope characteristics described within the terrane are mostly associated with crustal recycling with minor juvenile inputs (Santos *et al.* 2015 and references therein).

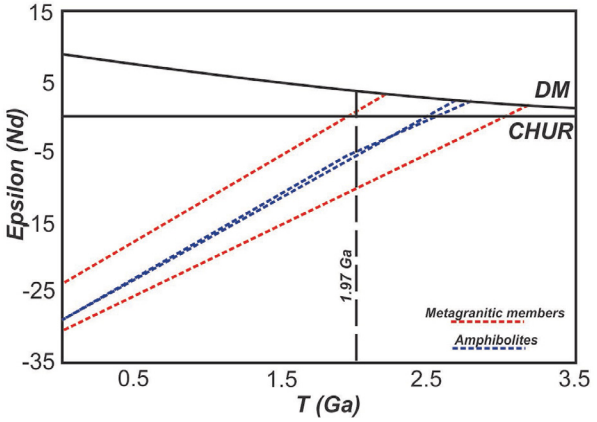

Figure 5. Nd evolution diagram for the studied rocks in the Sumé region.

Table 2. Summary of Nd isotope data for the metaplutonic rocks of the Sumé region. Samples SC-51, 14, and 05 stand for metagranitic members, whereas SC-78 corresponds to an amphibolite.

Sample	Sm (ppm)	Nd (ppm)	$^{143}Nd/^{144}Nd$	εNd (0)	εNd (t)	U-Pb age (Ga)	T_{DM} (Ga)
SC-51	20.05	1,333.5	0.511437	-23.43	-0.08	1.997	2.97
SC-14	1.02	5.17	0.511099	-30.02	-10.44	1.997	2.97
SC-05	7.67	48.01	0.510916	-30.17	-4.89	1.997	2.97
SC-78	5.58	32.21	0.511120	-29.61	-6.40	1.997	2.97

In both groups of rocks, trace elements signature share similarities with classical Phanerozoic "Arc-related magmas." Hence, we suggest that they were emplaced in a subduction-related setting. Our statement is mostly based on:

1. enrichment of LILE and depletion of HFSE;
2. prominent negative anomalies, such as Nb, Ta, besides low P and Ti;
3. the "arc-like to syn-collisional signature" recorded on discriminant diagrams (*e.g.*, Pearce 1982, Pearce *et al.* 1984, Harris *et al.* 1986, Agrawal *et al.* 2008).

Such pattern clearly characterizes depletion of HFSE in the source region, which can be explained by their low mobility compared to lithophile elements (Tatsumi *et al.* 1986). This geochemical behavior of trace elements is usually attributed to fluids released during dehydration of the subducting oceanic slab that migrates into the mantle wedge promoting partial melting by depressing *solidus* temperature (Tatsumi & Eggins 1995, Tatsumi 2005).

On the other hand, the depletion on Nb-Ta-Ti can also reflects the presence of rutile, sphene or Ti-bearing amphibole in the dehydrating slab during subduction, whereas significant

Table 3. Major (wt. %) and trace element (ppm) concentrations of studied metaigneous rocks, Alto Moxotó Terrane, NE Brazil.

Sample	SC05*	SC14*	SC27*	SC51*	SC71*	SC135A*	SC05B**	SC14**	SC34**	SC37**	SC71A**	SC78**	LSM75**
Major elements (wt.%)													
SiO_2	72.11	69.51	61.31	75.49	72.37	68.54	50	46.83	48.07	47.43	51.03	47.63	49.9
Al_2O_3	15.29	14.17	15.9	13.03	12.91	14.84	6.76	10.26	5.64	7.08	8.87	6.12	3.18
CaO	1.22	1.51	3.3	1.34	4.9	2.95	22.11	18.53	22.7	22.08	19.78	22.82	20.7
Fe_2O_3	0.051	0.82	2.06	1.19	1.09	2.18	5.9	11.13	6.78	7.91	6.53	8.54	9.43
FeO	0.045	0.74	1.85	1.07	0.98	1.96	5.31	10.02	6.1	7.12	5.88	7.69	8.48
K_2O	6.73	10.46	10.87	4.76	4.86	5.62	0.19	1	0.13	0.14	0.99	0.17	0.19
MgO	0.08	0.22	1.47	0.06	0.59	0.95	11.82	8.23	12.71	9.97	7.44	11.63	13.4
MnO	0.01	0.01	0.05	0.02	0.03	0.04	0.29	0.33	0.35	0.44	0.21	0.3	0.62
Na_2O	2.84	1.01	1.85	3.05	1.42	2.81	0.67	1.14	0.38	0.87	1.25	0.35	0.58
P_2O_5	0.05	0.06	0.3	0.03	0.22	0.18	n.d.	0.13	0.02	0.02	1.77	n.d.	0.01
TiO_2	0.04	0.65	0.07	0.06	0.06	0.14	0.25	0.53	0.38	0.24	0.3	0.54	0.26
Total	98	99	99	100	99	100	103	108	103	103	104	105	106
Trace elements (ppm)													
Ba	835	1917	2534	91	2317	1749	33	267	343	120	458	270	121
Ce	75	50.8	130.8	17.1	44.2	145.5	34.5	74	57.1	34	166.1	24.5	202.4
Dy	0.9	1.7	1.7	0.7	1	2.3	2.2	4	2.8	1.1	3.2	2.7	4.8
Er	0.3	0.9	0.6	0.4	0.5	1.1	1.1	1.9	1.2	0.5	1.7	1.4	2.3
Eu	1	0.7	0.5	0.4	0.4	1.2	0.6	0.9	1.2	1.4	1.1	0.5	1.7
Ga	16.5	11.7	14.2	15.3	13	17.3	12.5	16.1	11.3	13.6	18.1	8.9	9.1
Gd	1.5	2.1	2.9	0.7	1.7	3.4	2.7	4.9	4.3	1.1	4.6	2.3	6.4
Hf	0.3	8.2	1	1.5	1.1	2.3	4.2	1.8	2.3	3.5	2.1	1.7	1.8
Ho	0.1	0.3	0.3	0.1	0.2	0.4	0.4	0.8	0.5	0.2	0.6	0.5	0.9
La	74.3	21.6	44.2	9.2	25.7	88	12.9	32.4	50.2	17	81.1	10.7	94.4
Lu	0.1	0.1	0.1	0.1	0.1	0.1	0.2	0.3	0.2	0.1	0.3	0.2	0.3
Nb	1.2	3.2	2.8	4.4	1.9	2.9	2.2	6.8	1.6	0.7	5	0.7	0.4
Nd	29.5	20.7	36.3	6.5	17	48.1	20.2	32.1	46.5	12.6	58.5	14.4	68.3
Pr	9.9	5.6	10.3	1.8	4.9	15.2	4.9	8.7	12.5	13.7	16.6	3.4	20.2
Rb	200.4	285.5	354	82.8	106.3	98.6	4.5	30.8	4	3.5	21.1	6.7	3.7
Sm	3.1	3.4	5.4	1.1	2.4	5.8	3.7	6.1	6.9	2.1	7.5	2.7	9.7
Sn	n.d.	6	1	n.d.	n.d.	1	5	3	3	3	3	7	4
Sr	182.4	267.8	322.8	112.9	734.6	400.3	94.2	233.9	122.2	222	866.3	173.5	71.6
Ta	0.1	0.8	0.3	0.3	0.1	0.1	0.6	0.8	0.3	0.1	0.5	0.2	0.1
Tb	0.2	0.3	0.4	0.1	0.2	0.5	0.4	0.7	0.6	0.2	0.6	0.4	0.9
Th	4	16.3	13	4	8.3	28.7	2.3	3	1.7	1.2	4.44	0.9	1.8
Tm	0.1	0.2	0.1	0.1	0.1	0.1	0.2	0.3	0.2	0.1	0.3	0.2	0.3
U	0.4	1.7	1	1.3	0.8	0.8	0.7	0.8	0.3	0.1	3.7	0.6	0.8
V	n.d.	17	9	n.d.	35	40	45	91	50	65	61	150	88
Y	3.9	9.4	7.1	3.4	5.4	10.5	11.2	22.1	12.8	5.4	16.5	12.6	24.8
Yb	0.2	1	0.4	0.5	0.5	0.1	1.1	1.9	1.1	0.6	1.7	1.4	2.1

n.d.: not detected; *: metagranitic rocks; **: metamafic rocks.

depletion of HREE might also reflect certain amount of garnet as a residual phase (Foley *et al.* 2000, Klemme *et al.* 2006). Also, these geochemical features support fluid transport of trace elements under low pressure conditions (Baier *et al.* 2008). In addition, negative and positive Eu anomalies are consistent with residual plagioclase in the source and anomalous accumulation of this mineral in the melt, that can be ascribed to fractional crystallization.

Similar petrographical and geochemical aspects are also observed in several metaplutonic rocks attributed to a major Rhyacian-Orosirian orogeny described for the AMT (*e.g.*, Brito Neves 2011, Brito Neves *et al.* 2014, Santos *et al.* 2017b). Indeed, the geochemical and isotopic signatures of the studied metamafic rocks are very similar to those from Carmo mafic-ultramafic suite, investigated just a few kilometers from the study area (Santos *et al.* 2015). On the other hand, high SiO_2, Al_2O_3 and K_2O contents of the studied granitic rocks suggest a more evolved stage of the magmatic arc. Such parameters are adequate for such interpretations, once that their protoliths were already potassic in nature (K-feldspar-rich members) and might explain the obtained younger age (c. 1.97 Ga). In addition, some samples plot in the syn-collisional field from Pearce *et al.* (1984) and are slightly peraluminous, indicating that they also might be associated with a final stage of continent-continent collision. Such hypothesis is in agreement with the late Paleoproterozoic obtained U-Pb age and the evidence of crust reworking provided by Nd data (Floresta Suite, Pedra d'Água Suite, Cabaceiras Complex, among others; Santos *et al.* 2017a and references therein). However, nature and conditions of continent-continent collision in the AMT still needs further investigations and must be expanded to other portions of the domain, mainly due to the scarcity of geochronological and isotope data.

Lastly, based on the combination of our data and those from the literature, we conclude that, after a major Neoarchean crustal growth event (Neves *et al.* 2015, Santos *et al.* 2017b and references therein), the AMT was strongly affected by a Paleoproterozoic accretion-collisional event that reworked previous crust. This event is characterized by the development of a long-lived continental magmatic arc, in which the studied potassic rocks record an evolved stage of it. Finally, we suggest that such magmatism spanned the Rhyacian and the Orosirian periods (*i.e.*, 2.15 – 1.97 Ga).

Stratigraphic implications and regional correlations

The studied rocks crop out in the type area of the Sumé Complex, described by Medeiros and Torres (2000) as a Neoproterozoic unit based on the available U-Pb from Silva *et al.* (2002). Rocks attributed to this sequence cover a large petrographic range (orthogneisses, migmatites, mafic rocks, paragneisses, schists and calc-silicate rocks) and are widespread throughout the AMT, being dubiously placed in the Neoproterozoic. However, in this study, as mentioned, a metagranitic rock that is attributed to this complex yielded a Paleoproterozoic age (*ca.* 1.97 Ga), which is coherent with several recently published geochronological/isotopic data available for the region that stands for the predominance of Paleoproterozoic crust (Neves *et al.* 2015, Santos *et al.* 2015, 2017b).

Due to the abundance of Rhyacian/Orosirian ages for the major units of the AMT in the recently published studies, besides the new U-Pb age obtained in this study, we suggest that the

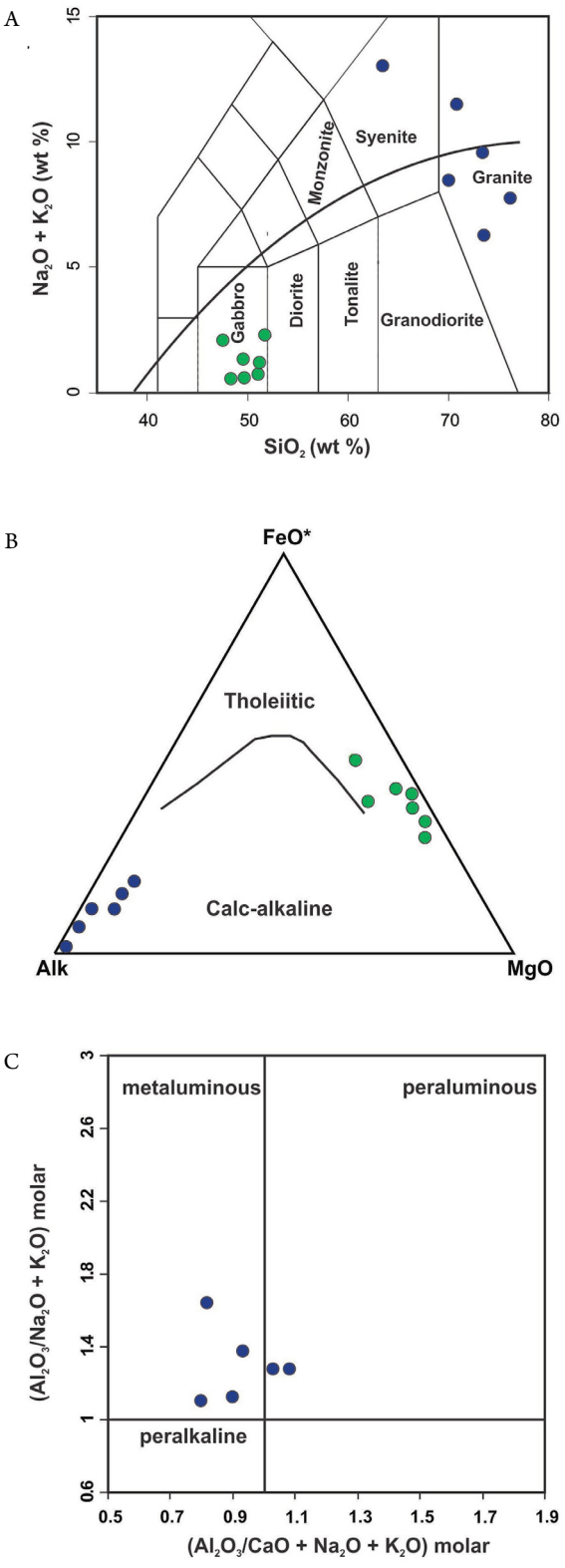

Figure 6. Major element plots for the studied samples (data from Table 3). (A) TAS diagram ($Na_2O + K_2O$ *vs.* SiO_2), from Le Bas *et al.* (1986); (B) AFM diagram from Irvine and Baragar (1971); (C) A/NK *vs.* ASI diagram, from Maniar and Picolli (1989), using Shand's index. Blue circles are metagranitic rock samples, and green circles represent metamafic rock samples.

use of the term *Sumé Complex* as a Neoproterozoic unit should be avoided. The duality of crustal ages within the AMT is not only found in these rocks. For instance, the Sertânia Complex (garnet-bearing paragneisses, garnet-sillimanite-biotite schists and migmatites) is another important unit exposed in the terrane, considered Paleoproterozoic in age by many authors, including Santos *et al.* (2004). Recently, Neves *et al.* (2017) documented Neoproterozoic zircon grains in metasedimentary rocks attributed to this unit, interpreting them as the maximum deposition age of the sedimentary pile. Hence, one must consider that it is possible that Neoproterozoic sequences can be distributed and deposited throughout major Paleoproterozoic units that formed the basement of the Borborema Province, being later deformed and metamorphosed together during the Brasiliano Orogeny, further complicating the original stratigraphic relations.

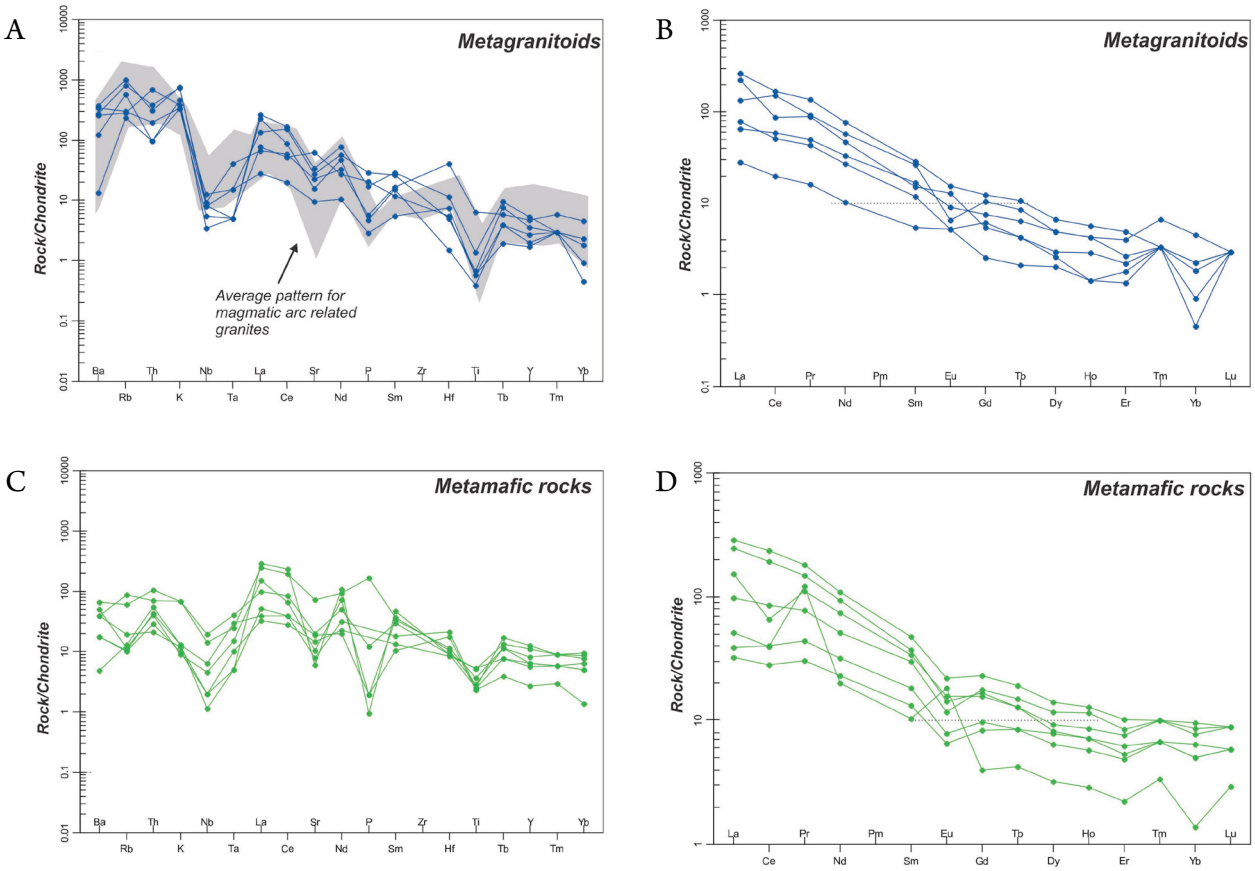

Figure 7. Chondrite-normalized spider diagrams (A) and (C) and rare earth elements (REE) patterns for the studied rocks (B) and (D). Standardization followed Nakamura (1974) normalizing values. Symbols are as in Figure 6.

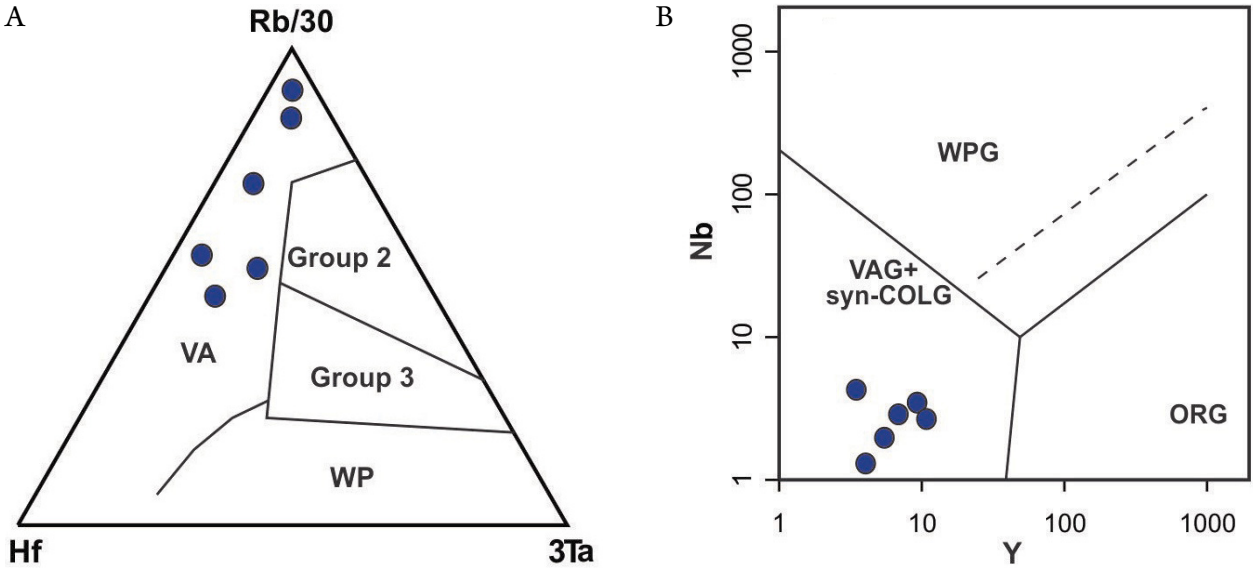

Figure 8. Discriminant diagrams of the studied rocks. (A) Hf-Rb/30-3Ta plot after Harris *et al.* (1986); (B) Y *vs.* Nb after Pearce *et al.* (1984). Fields indicate syn-collisional granites (syn-COLG), within-plate granites (WPG), volcanic arc-related granites (VAG) and ocean-ridge granites (ORG).

Although Rhyacian rocks are common and widespread in the Atlantic shield (in effect composing the majority of it), Orosirian rocks, on the other hand, are quite scarce, and might represent a magmatic event that was not previously considered in its full importance until recent times. In effect, in the southern Borborema Province, in the basement of the Rio Preto Fold belt, Caxito *et al.* (2015) recognized the first well described Orosirian rocks of the region, amphibolites which were then interpreted as developed in a supra-subduction zone setting, much like our interpretation for the Sumé Complex. The recognition of Orosirian fragments in both the southern and central Borborema Province might provide clues to a previously undetected important tectonic scenario, which deserves further studies and investigation.

On the other hand, older correlatives of the studied rocks are widespread in the province, Pan African Mobile belts and adjoining cratons. In central Borborema Province, they can be related to other subduction-related suites and coeval metamorphism. For instance, in other areas of the Transversal sub-province, Neves *et al.* (2015) described juvenile inputs of ca. 2.1 Ga, followed by 2.0 to 1.98 Ga continent-continent collision, crustal reworking and coeval metamorphism. A similar scenario is also observed in the northern sub-province: Rhyacian to Orosirian metagranitic rocks of the Troia Massif are related to accretionary and collisional tectonics at 2.1 and 2.0 Ga, respectively (Costa *et al.* 2015), whereas Paleoproterozoic reworking is also present in preserved Archean domains, such as the São José do Campestre (Dantas *et al.* 2013) and Granjeiro terrane (Silva *et al.* 2014).

Reworking of Archean basement resulted from collisional magmatism and coeval metamorphism is also recorded on metagranitic and gneissic-migmatitic suites of the São Francisco-Congo and São Luis-West Africa cratons (Barbosa & Sabaté 2004, Klein *et al.* 2012, among others). In the Pan-African mobile belts, preexisting crust, including TTG-like rocks, calc-alkaline and potassic rock suites are also widespread,

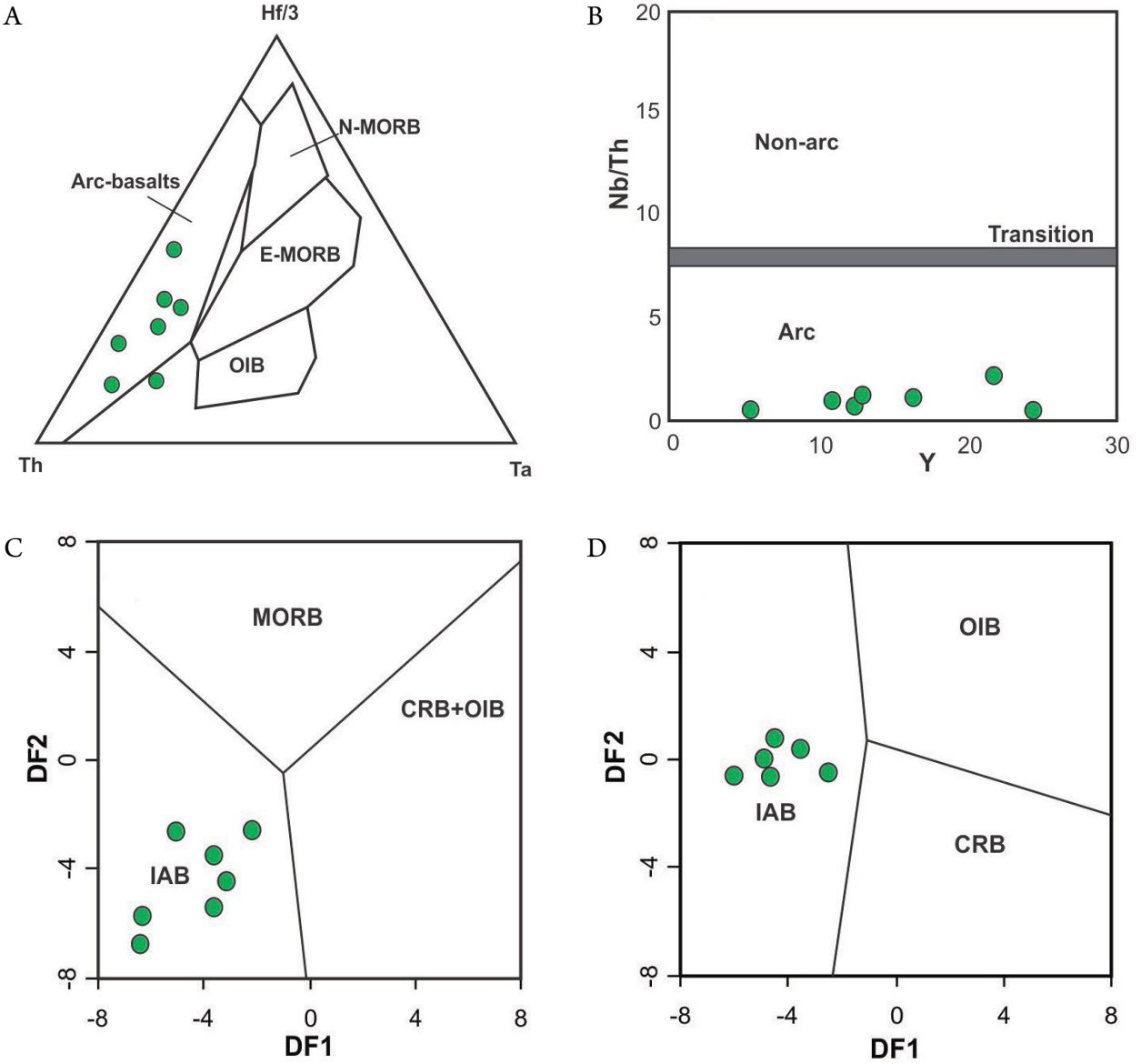

Figure 9. Discriminant diagrams of the studied rocks of the Sumé Complex. (A) Hf/3-Th-Ta plot after Wood (1980), Nb/Th *vs.* Y plot after Jenner *et al.* (1991); (B) and (C) discriminant functions DF1 *vs.* DF2 plot from Agrawal *et al.* (2008). Fields indicate mid-ocean ridge basalts (MORB and N-MORB), enriched mid ocean ridge basalts (E-MORB), ocean island basalts (OIB), island arc basalts (IAB) and continental rift basalts (CRB). Symbols are as in Figure 6.

mostly interpreted as originated via subduction-related tectonics. In most cases, such associations have been referred to be the result of long-lived Paleoproterozoic magmatism attributed to the Eburnean orogeny, similar to that observed within the AMT (*e.g.*, Penaye *et al.* 2004, Dada 2008, Baratoux *et al.* 2011, Block *et al.* 2016).

CONCLUSIONS

The main conclusions of this paper are:

1. Metaigneous rocks that occur in the Sumé region comprise monzogranites, syenogranites, alkali-feldspar granites, amphibolites, fine-grained metagabros and minor pyroxenites. These rocks have been recently attributed to the Neoproterozoic Sumé Complex. However, our obtained U-Pb age of 1.97 Ga of a metasyenogranitic rock, as well as similar geochemical and isotopic characteristics of the studied mafic rocks and other Paleoproterozoic suites within the terrane, indicates that this set of rocks is in fact Rhyacian to Orosirian in age;
2. Based on geochemical and Sm-Nd isotope characteristics, we suggest that such rocks are associated with a major Paleoproterozoic orogeny (*ca.* 2.1 – 1.9 Ga), that is described in the central Borborema Province. The magmagenesis involved reworking of previously formed crust, with sources that range from to Mesoarchean to early Paleoproterozoic;
3. The obtained results are compatible with other Paleoproterozoic belts of the Borborema Province, adjoining cratons and West African mobile belts underlying Nigeria and Cameroon. Such correlations demonstrate the importance in investigating Paleoproterozoic crustal segments within Neoproterozoic belts of Western Gondwana, providing clues for paleogeographic reconstructions. However, Orosirian magma genesis is quite scarce, and its significance must be considered in regional correlations/interpretations.

ACKNOWLEDGEMENTS

One of the major retirement plans of Edilton José dos Santos was to write a manuscript concerning the nature of the Sumé Complex and its role in the AMT evolution. Unfortunately, he did not live enough to it, and Lauro Cézar Montefalco de Lira Santos felt that he had to move on with this topic. The final result is this paper, which is Lira Santos' personal tribute to him. Christian Carmona, Cesar Verissimo and Adauto Neto are thanked for the geochemical data concession. Elton Dantas and Benjamin Bley are equally thanked for providing facilities on isotope data acquisition, and Reinhardt Fuck and Geysson Lages are thanked for early discussion. The authors also would like to express gratitude to Editor Claudio Riccomini, as well as Fabricio Caxito and the anonymous reviewers for their criticism and suggestions that helped improve the original manuscript. This is a late contribution to the Project *O Magmatismo Anorogênico Pré-Cariris Velhos na Região de Sumé e Camalaú (PB) e seu significado na Evolução da Província Borborema*, granted to Edilton José dos Santos in 2008 by the Brazilian Council for Scientific and Technological Development (CNPq).

ARTICLE INFORMATION

Manuscript ID: 20180083. Received on: 07/26/2018. Approved on: 12/07/2018.

E. J. S. wrote a preliminary draft of the manuscript, collected the data and formulated the former ideas regarding the geology of the Sumé area and the AMT as well. L. C. M. L. S. contributed with the figures, tables, data interpreting, final geological model, reshaping of the text, as well as took care of all the submitting phases, once that, unfortunately, the first author passed away early in the submission year.

Competing interests: The authors declare no competing interests.

REFERENCES

Agrawal S., Guevara M., Verma S.P. 2008. Tectonic discrimination of basic and ultrabasic volcanic rocks through log-transformed ratios of immobile trace elements. *International Geology Review*, **50**(12):1057-1079. http://doi.org/10.2747/0020-6814.50.12.1057

Almeida F.F.M., Hasui Y., Brito Neves B.B., Fuck R.A. 1981. Brazilian structural provinces: an introduction. *Earth Science Reviews*, **17**(1-2):1-21. http://doi.org/10.1016/0012-8252(81)90003-9

Baier J., Audétat A., Keppler H. 2008. The origin of the negative niobium tantalum anomaly in subduction zone magmas. *Earth and Planetary Science Letters*, **267**(1-2):290-300. http://doi.org/10.1016/j.epsl.2007.11.032

Baratoux L., Metelka V., Naba S., Jessel W.M., Gregorie M., Ganne J. 2011. Juvenile paleoproterozoic crust Evolution during the Eburnean orogeny (2.2-2.0 Ga), western Burkina Faso. *Precambrian Research*, **191**(1-2):18-45. http://doi.org/10.1016/j.precamres.2011.08.010

Barbosa J.S.F., Sabaté P. 2004. Archaean and paleoproterozoic crust of the São Francisco craton, Bahia, Brazil: geodynamic features. *Precambrian Research*, **133**(1-2):1-27. http://doi.org/10.1016/j.precamres.2004.03.001

Basto C.F., Caxito F.A., Vale J.A.R., Silveira D.A., Rodrigues J.B., Alkmin A.R., Valeriano C.M., Santos E.J. 2019. An Ediacaran back-arc basin preserved in the Transversal Zone of the Borborema Province: Evidence from geochemistry, geochronology and isotope systematics of the Ipueirinha Group, NE Brazil. *Precambrian Research*, **320**:213-231. http://doi.org/10.1016/j.precamres.2018.11.002

Block S., Baratoux L., Zeh A., Laurent O., Bruguier O., Jessell M., Ailleres L., Sagna R., Parra-Avila L.A., Bosch D. 2016. Paleoproterozoic juvenile crust formation and stabilisation in the south-eastern West African Craton (Ghana); new insights from UPb–Hf zircon data and geochemistry. *Precambrian Research*, **287**:1-30. http://doi.org/10.1016/j.precamres.2016.10.011

Brito Neves B.B. 2011. The Paleoproterozoic in the South American continent: diversity in the geologic time. *Journal of South American Earth Sciences*, **32**(4):270-286. http://doi.org/10.1016/j.jsames.2011.02.004

Brito Neves B.B., Fuck R.A., Pimentel M.M. 2014. The Brasiliano collage in South America: a review. *Brazilian Journal of Geology*, **44**(3):493-518. http://doi.org/10.5327/Z2317-4889201400030010

Brito Neves B.B., Santos E.J., Schmus W.R.Q. 2000. Tectonic history of the Borborema province. *In*: Cordani U., Milani E.J., Thomaz Filho A., Campos D.A. (Eds.). *Tectonic Evolution of South America*. Rio de Janeiro: 31st International Geological Congress, p. 151-182.

Brown M. 2006. Duality of thermal regimes is the distinctive characteristic of plate tectonics since the Neoarchean. *Geology*, **34**(11):961-964. http://doi.org/10.1130/G22853A.1

Bühn B.M., Pimentel M.M., Matteini M., Dantas E.L. 2009. High spatial resolution analysis of Pb and U isotopes for geochronology by laser ablation multicollector inductively coupled plasma mass spectrometry (LA-MC-ICP-MS). *Anais da Academia Brasileira de Ciências*, **81**(1):1-16. http://doi.org/10.1590/S0001-37652009000100011

Cawood P.A., Hawkesworth C.J., Dhuime B. 2013. The continental record and the generation of continental crust. *Geological Society of America Bulletin*, **125**(1-2):14-32. http://doi.org/10.1130/B30722.1

Cawood P.A., Kröner A., Collins W.J., Kusky T.M., Mooney W.D., Windley B.F. 2009. Accretionary orogens through earth history. *Geological Society of London Special Publication*, **318**(1):1-36. http://doi.org/10.1144/SP318.1

Caxito F.A., Uhlein A., Dantas E.L., Stevenson R., Pedrosa-Soares A.C. 2015. Orosirian (ca. 1.96 Ga) mafic crust of the northwestern São Francisco Craton margin: Petrography, geochemistry and geochronology of amphibolites from the Rio Preto fold belt basement, NE Brazil. *Journal of South American Earth Sciences*, **59**:95-111. http://doi.org/10.1016/j.jsames.2015.02.003

Caxito F.A., Uhlein A., Dantas E.L., Stevenson R., Salgado S.S., Dussian I.A., Sial A.N. 2016. A complete Wilson Cycle recorded within the Riacho do Pontal Orogen, NE Brazil: Implications for the Neoproterozoic evolution of the Borborema Province at the heart of West Gondwana. *Precambrian Research*, **282**:97-120. http://doi.org/10.1016/j.precamres.2016.07.001

Costa F.G., Klein E.L., Lafon J.M., Milhomem Neto J.M., Galarza M.M., Rodrigues J.B., Naleto J.L.C., Lima R.G.C. 2018. Geochemistry and U–Pb–Hf zircon data for plutonic rocks of the Troia Massif, Borborema Province, NE Brazil: Evidence for reworking of Archean and juvenile Paleoproterozoic crust during Rhyacian accretionary and collisional tectonics. *Precambrian Research*, **311**:167-194. http://doi.org/10.1016/j.precamres.2018.04.008

Costa F.G., Palheta E.S.M., Rodrigues J.B., Gomes I.P., Vasconcelos A.M. 2015. Geochemistry and U-Pb zircon ages of plutonic rocks from the Algodões granite–greenstone terrane, Troia Massif, northern Borborema Province, Brazil: implications for Paleoproterozoic subduction–accretion processes. *Journal of South American Earth Sciences*, **59**:45-68. http://doi.org/10.1016/j.jsames.2015.01.007

Dada S.S. 2008. Proterozoic Evolution of the Nigeria-Borborema province. *Geological Society of London Special Publication*, **294**(1):121-136. http://doi.org/10.1144/SP294.7

Dantas E.L., Souza Z.S., Wernick E., Hackspacher P.C., Martin H., Xiadong D., Li J.W. 2013. Crustal growth in the 3.4-2.7 Ga São Jose do Campestre Massif, Borborema province, NE Brazil. *Precambrian Research*, **227**:120-156. http://doi.org/10.1016/j.precamres.2012.08.006

De Wit M.J., Stankiewicz J., Reeves C. 2008. Restoring Pan-African Brasiliano connections: more Gondwana control, less Trans-Atlantic comparison. *In*: Pankhurst R.J., Trouw R.A.J., Brito Neves B.B., de Wit M.J. (Eds.). *West Gondwana Pre-Cenozoic Correlations Across the South Atlantic Region*. London, Geological Society Special Publication, v. 294, p. 399-412.

DePaolo D.J. 1981. Neodymium isotopes in the Colorado front range and crust-mantle evolution in the Proterozoic. *Nature*, **291**:193-196.

Foley S.F., Barth M.G., Jenner G.A. 2000. Rutile/melt partition coefficient for trace elements and an assesment of the influence of rutile on the trace element characteristics of subduction zone magmas. *Geochemica et Cosmochimica Acta*, **64**(5):933-938. http://doi.org/10.1016/S0016-7037(99)00355-5

Ganade C.E., Basei M.A.S., Grandjean F.C., Armstrong R., Brito R.S. 2017. Contrasting Archaean (2.85–2.68 Ga) TTGs from the Tróia Massif (NE-Brazil) and their geodynamic implications for flat to steep subduction transition. *Precambrian Research*, **297**:1-18. http://doi.org/10.1016/j.precamres.2017.05.007

Harris N.B.W., Pearce J.A., Tindle A.G. 1986. Geochemical characteristics of collision zone magmatism. *In*: Coward M.P., Reis A.C. (Eds.). *Collision Tectonics*. Geological Society Special Publication, v. 19, p. 67-81.

Hawkesworth C.J., Cawood P.A., Dhuime B., Kemp T.I.S. 2017. Earth's continental lithosphere through time. *Annual Review of Earth and Planetary Sciences*, **45**:169-198. http://doi.org/10.1146/annurev-earth-063016-020525

Hawkesworth C.J., Kemp A.I.S. 2006. Evolution of the continental crust. *Nature*, **443**:811-817. http://doi.org/10.1038/nature05191

Hong E., Kao W. 2015. Unraveling the formation of continental crust: a review and outlook. *Journal of Marine Science and Technology*, **23**(4):575-578. http://doi.org/10.6119/JMST-015-0416-2

Irvine T.N., Baragar W.R.A. 1971. A guide to chemical classification of the common volcanic rocks. *Canadian Journal of Earth Sciences*, **8**(5):523-548. https://doi.org/10.1139/e71-055

Jackson S.E., Pearson N.J., Griffin W.L., Belousova E.A. 2004. The application of laser ablation-inductively coupled plasma-mass spectrometry to in situ U-Pb zircon geochronology. Chemical Geology, **211**(1-2):47-69. http://doi.org/10.1016/j.chemgeo.2004.06.017

Jenner G.A., Dunning G.R., Malpas J., Brown M., Brace T. 1991. Bay of Islands and Little Port Complexes, revisited: age, geochemical and isotopic evidence confirm suprasubduction zone origin. *Canadian Journal of Earth Science*, **28**(10):1635-1652. https://doi.org/10.1139/e91-146

Klein E.L., Rodrigues J.B., Lopes E.C.S., Soledade G.L. 2012. Diversity of Rhyacian granitoids in the basement of the Neoproterozoic-Early Cambrian Gurupi Belt, northern Brazil: Geochemistry, U-Pb zircon geochronology, and Nd isotope constraints on the Paleoproterozoic magmatic and crustal evolution. *Precambrian Research*, **220-221**:192-216. http://doi.org/10.1016/j.precamres.2012.08.007

Klemme S., Günther D., Hametner K., Prowatke S., Zack T. 2006. The partitioning of trace elements between ilmenite, ulvospinel, armalcolite and silicate melts with implications for the early differentiation of the moon. *Chemical Geology*, **234**(3-4):251-263. http://doi.org/10.1016/j.chemgeo.2006.05.005

Le Bas M.J., Le Maitre R.W., Streckeisen A., Zanettin B. 1986. A chemical classification of volcanic rocks based on the total alcali-silica diagram. *Journal of Petrology*, **27**(3):745-750. https://doi.org/10.1093/petrology/27.3.745

Magdanelo G.B., Petronilho L.A., Silva R.A., Ruiz I.R., Babisnki M., Hollanda M.H.B.M., Martins V.T.S. 2017. Pb-Sr-Nd Isotopic characterization of USGS reference materials by TIMS at CPGeo-USP. *In*: Workshop of Inorganic Mass Spectrometry, 2. *Abstracts*.

Maniar P.D., Piccoli P.M. 1989. Tectonic discrimination of granitoids. *Geological Society of America Bulletin*, **101**(5):635-643. https://doi.org/10.1130/0016-7606(1989)101%3C0635:TDOG%3E2.3.CO;2

Martin H., Smithies R.H., Rapp R., Moyen J.F., Champion D. 2005. An overview of adakite, TTG and sanukitoid: relationships and some implications for crustal evolution. *Lithos*, **79**(1-2):1-24. https://doi.org/10.1016/j.lithos.2004.04.048

Matteini M., Junges S.L., Dantas E.L., Pimentel M.M., Bühn B.M. 2010. In situ zircon U-Pb and Lu-Hf isotope systematic on magmatic rocks: insights on the crustal evolution of the Neoproterozoic Goias Magmatic Arc, Brasília belt, Central Brazil. *Gondwana Research*, **17**(1):1-12. http://doi.org/10.1016/j.gr.2009.05.008

Medeiros V.C., Torres H.H.F. 2000. *Programa Levantamentos Geológicos Básicos do Brasil*. Sumé. Folha SB.24-Z-D-V. Estados da Paraíba e Pernambuco. Falcão Torres. Escala 1:100.000. Brasília, CPRM. 1 CD-ROM.

Meert J.G. 2012. What's in a name? The Columbia (Paleopangaea/Nuna) supercontinent. *Gondwana Research*, **21**(4):987-993. http://doi.org/10.1016/j.gr.2011.12.002

Nakamura N. 1974. Determination of REE, Ba, Fe, Mg, Na and K in carbonaceous and ordinary chondrites. *Geochemhimica et Cosmochimica Acta*, **38**(5):757-775. https://doi.org/10.1016/0016-7037(74)90149-5

Nascimento M.A., Galindo A.C., Medeiros V.C. 2015. Ediacaran to Cambrian magmatic suites in the Rio Grande do Norte domain, extreme Northeastern Borborema Province (NE of Brazil): Current knowledge. *Journal of South American Earth Sciences*, **58**:281-299. https://doi.org/10.1016/j.jsames.2014.09.008

Neves S.P. 2015. Constraints from zircon geochronology on the tectonic evolution of the Borborema Province (NE Brazil): widespread intracontinental Neoproterozoic reworking of a Paleoproterozoic accretionary orogen. *Journal of South American Earth Sciences*, **58**:150-164. https://doi.org/10.1016/j.jsames.2014.08.004

Neves S.P., da Silva J.M.R., Bruguier O. 2017. Geometry, kinematics and geochronology of the Sertânia Complex (central Borborema Province, NE Brazil): Assesing the role of accretionary versus intraplate processes during West Gondwana assembly. *Precambrian Research*, **298**:552-571. http://doi.org/10.1016/j.precamres.2017.07.006

Neves S.P., Lages G.A., Brasilino R.G., Miranda A.W.A. 2015. Paleoproterozoic accretionary and collisional processes and the build-up of the Borborema Province (NE Brazil): geochronological and geochemical evidence from the Central Domain. *Journal of South American Earth Sciences*, **58**:165-187. http://doi.org/10.1016/j.jsames.2014.06.009

Pearce J.A. 1982. Trace elements characteristics of lavas from destructive plate boundaries. *In*: Thorpe R.S. (Ed.). *Andesites*. London, John Wiley and Sons, p. 525-548.

Pearce J.A., Harris N.B.W., Tindle A.G. 1984. Trace element discrimination diagrams for the tectonic interpretation of granitic rocks. *Journal of Petrology*, **25**(Part 4):956-983.

Penaye J., Toteu S.F., Tchameni R., Van Schmus W.R., Tchakounté J., Ganwa A., Minyem D., Nsifa E.N. 2004. The 2.1 Ga West Central African Belt in Cameroon: extension and evolution. *Journal of African Earth Sciences*, **39**(3-5):159-164. http://doi.org/10.1016/j.jafrearsci.2004.07.053

Rudnick R.L. 1995. Making continental crust. *Nature*, **378**:571-578. https://doi.org/10.1038/378571a0

Santos E.J., Medeiros V.C. 1999. Constraints from granitic plutonism on proterozoic crustal growth of the Transverse Zone, Borborema Province, NE-Brazil. *Revista Brasileira de Geociências*, **29**(1):73-84. http://doi.org/10.25249/0375-7536.1999297384

Santos E.J., Nutman A.P., Brito Neves B.B. 2004. Idades SHRIMP U-Pb do Complexo Sertânia: Implicações sobre a evolução tectônica da Zona Transversal, Província Borborema. *Geologia USP: Série Científica*, **4**(1):1-12. https://doi.org/10.5327/S1519-874x2004000100001

Santos E.J., Van Schmus W.R., Kozuch M., Brito Neves B.B. 2010. The Cariris Velhos tectonic event in northeast Brazil. *Journal of South American Earth Sciences*, **29**(1):61-76. http://doi.org/10.1016/j.jsames.2009.07.003

Santos L.C.M.L., Dantas E.L., Cawood P.A., Lages G.A., Lima H.M., Santos E.J. 2018. Accretion Tectonics in Western Gondwana deduced from Sm-Nd Isotope mapping of terranes in the Borborema Province, NE Brazil. *Tectonics*, **37**:2727-2743. https://doi.org/10.1029/2018TC005130

Santos L.C.M.L., Dantas E.L., Cawood P.A., Santos E.J., Fuck R.A. 2017a. Neoarchean crustal growth and Paleoproterozoic reworking in the Borborema Province, NE Brazil: insights from geochemical and isotopic data of TTG and metagranitic rocks of the Alto Moxotó Terrane. *Journal of South American Earth Sciences*, **79**:342-363. http://doi.org/10.1016/j.jsames.2017.08.013

Santos L.C.M.L., Dantas E.L., Santos E.J., Santos R.V., Lima H.M. 2015. Early to late Paleoproterozoic magmatism in NE Brazil: The Alto Moxotó Terrane and its tectonic implications for the pre-West Gondwana assembly. *Journal of South American Earth Sciences*, **58**:188-209. http://doi.org/10.1016/j.jsames.2014.07.006

Santos L.C.M.L., Dantas E.L., Vidotti R.M., Cawood P.A., Santos E.J., Fuck R.A., Lima H.M. 2017b. Two-stage terrane assembly in Western Gondwana: Insights from structural geology and geophysical data of central Borborema Province, NE Brazil. *Journal of Structural Geology*, **103**:167-184. http://doi.org/10.1016/j.jsg.2017.09.012

Silva L.C. 2006. *Geocronologia aplicada ao mapeamento regional, com ênfase na técnica U-Pb SHRIMP e ilustrada com estudos de casos brasileiros*. Brasília, CPRM, 150 p. (Publicações Especiais do Serviço Geológico do Brasil; 1). Available at: <www.cprm.gov.br>. Accessed on: July 24, 2018.

Silva L.C., Armstrong R., Pimentel M.M, Scandolara J., Ramgrab G., Wildner W., Angelim L.A.A., Vasconcelos A.M., Rizzoto G., Quadros M.L.E.S., Sander A., Rosa A.L.Z. 2002. Reavaliação da evolução geológica em terrenos pré-cambrianos brasileiros com base me novos dados U-Pb SHRIMP, Parte III: Províncias Borborema, Mantiqueira Meridional e Rio Negro-Juruena. *Revista Brasileira de Geociências*, **32**(4):529-544.

Silva L.C., Costa F.G., Armstrong R., McNaugthon N.J. 2014. U–Pb (SHRIMP) zircon dating and Nd isotopes at basement inliers from northern Borborema Province, Ceará State, NE Brazil: evidences for the Archean and Paleoproterozoic crustal evolution. *In*: South American Symposium on Isotope Geology, 9., São Paulo, Brazil. *Abstracts …*, p. 175.

Tatsumi Y. 2005. The subduction factory: How it operates in the evolving Earth? *GSA Today*, **15**(7):4-10. http://dx.doi.org/10.1130/1052-5173(2005)015[4:TSFHIO]2.0.CO;2

Tatsumi Y., Eggins S. 1995. *Subduction zone magmatism*. Boston, Blackwell Science.

Tatsumi Y., Hamilton D.L., Nesbitt R.W. 1986. Chemical characteristics of fluid phase released from a subducted lithosphere and origin of arc magmas: evidence from high pressure experiments of natural rocks. *Journal of Volcanology and Geothermal Research*, **29**(1-4):293-309. https://doi.org/10.1016/0377-0273(86)90049-1

Van Schmus W.R., Kozuch M., Brito Neves B.B. 2011. Precambrian history of the zona transversal of the Borborema Province. *Journal of South American Earth Sciences*, **31**(2-3):227-252. http://doi.org/10.1016/j.jsames.2011.02.010

Vaughan A.P.M., Leat P.T., Pankhurst R.J. 2005. Terrane processes at the margins of Gondwana: introduction. *Geological Society of London Special Publication*, **246**(1):1-21. http://doi.org/10.1144/GSL.SP.2005.246.01.01

Wood D.A. 1980. The application of a Th-Hf-Ta diagram to problems of tectonomagmatic classification and to establishing the nature of crustal contamination of basaltic lavas of the British Tertiary volcanic province. *Earth and Planetary Science Letters*, **50**(1):11-30. http://dx.doi.org/10.1016/0012-821X(80)90116-8

Zhao G.C., Sun M., Wilde S.A., Sanzhong L. 2004. Paleo-Mesoproterozoic supercontinent: assembly, growth and breakup. *Earth Science Reviews*, **67**(1-2):91-123. http://doi.org/10.1016/j.earscirev.2004.02.003